Single-Molecule Optomechanical Cycle
Thorsten Hugel, *et al.*
Science **296**, 1103 (2002);
DOI: 10.1126/science.1069856

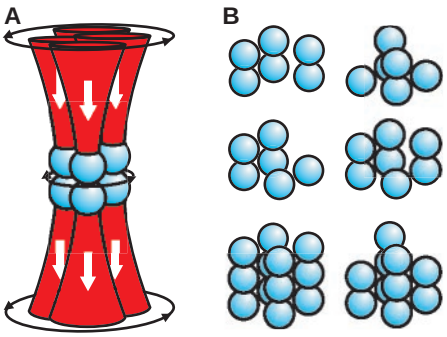

Fig. 4. (**A**) The geometry of the interference pattern that leads to the data of Fig. 3, B and C. (**B**) Diagrams of various other trapped structures, including asymmetric structures, which we have assembled experimentally in our optical tweezers.

between two light beams for the controlled rotation of an interference pattern. This technique can be applied in any situation where slow motion of an interference pattern is desired, such as translating particles in simple linear interferometric tweezers (*20*) or creating a moving "conveyor belt" of dipole traps for deterministic delivery of ensembles of cold atoms (*21*).

The angular Doppler effect makes use of the fact that circularly polarized light reverses its handedness when passing through a half-wave plate. Thus a change in spin angular momentum of $2\hbar$ per photon occurs as the light passes through this optical element. If the wave plate now rotates, energy can be exchanged between the rotating plate and the light beam, causing either an increase or decrease in the frequency of the light beam (*22*). In our system, a rotating half-wave plate is used, but this could be replaced by an electro-optic crystal to mimic this effect and therefore offers a system that would have no moving parts.

Different versions of the interference pattern between two LG beams of opposite helicity have been used for studies of various groups of trapped particles. The pattern is directed, in our tweezers geometry, into a sample cell containing 1-μm silica spheres dispersed in water. Using a pattern formed by superimposing an $l = 1$ beam onto an $l = -1$ beam (two spots), we have tweezed and rotated several rodlike particles including chromosomes. Groups of spheres have been rotated and simultaneously translated vertically through the sample slide, thus giving full 3D control (Fig. 3A). Interfering an $l = 2$ and $l = -2$ LG beam creates a 3D light intensity distribution suitable for the creation of cubic structures (Fig. 3B and Fig. 4A). By adjusting the sample stage, we were able to tweeze particles into the bright regions, forming four separate stacks, each with two spheres, creating a 3D cubic structure (Fig. 3B). In Fig. 3B, the light beam is blocked and the 3D structure (seen complete in the first frame) collapses to reveal the eight constituent 1-μm (in diameter) spheres. The structure is rotated using the angular Doppler effect (Fig. 3C). We also stacked additional particles in each bright region, creating different cubic structures. By controlling the number of spheres loaded in each bright region, we created asymmetric 3D structures (Fig. 4B). Our propagating interference pattern can be combined with a standing wave to offer discrete trapping sites in the axial direction (*23*). The creation and manipulation of artificial structures (such as those in Fig. 4B) at or just below the micrometer level is of current interest in colloid physics. Our ensemble of trapped particles can act as a predetermined nucleus for subsequent growth of novel crystalline structures by self-assembly.

References and Notes

1. A. Ashkin, J. M. Dziedzic, J. E. Bjorkholm, S. Chu, *Opt. Lett.* **11**, 288 (1986).
2. A. Ashkin, J. M. Dziedzic, T. Yamane, *Nature* **330**, 769 (1987).
3. S. B. Smith, Y. Cui, C. Bustamante, *Science* **271**, 795 (1996).
4. M. E. J. Friese, T. A. Nieminen, N. R. Heckenberg, H. Rubinsztein-Dunlop, *Nature* **394**, 348 (1998).
5. E. Higurashi, R. Sawada, T. Ito, *Phys. Rev. E* **59**, 3676 (1999).
6. N. B. Simpson, K. Dholakia, L. Allen, M. J. Padgett, *Opt. Lett.* **22**, 52 (1997).
7. P. Galajda, P. Ormos, *Appl. Phys. Lett.* **78**, 249 (2001).
8. L. Paterson *et al.*, *Science*, **292**, 912 (2001).
9. E. R. Dufresne, G. C. Spalding, M. T. Dearing, S. A. Sheets, D. G. Grier, *Rev. Sci. Instrum.* **72**, 1810 (2001).
10. R. L. Eriksen, P. C. Mogensen, J. Glückstad, *Opt. Lett.* **27**, 267 (2002).
11. P. Zemánek, A. Jónaš, L. Šrámek, M. Liška, *Opt. Lett.* **24**, 1448 (1999).
12. J. Arlt, V. Garcés-Chávez, W. Sibbett, K. Dholakia, *Opt. Commun.* **197**, 239 (2001).
13. R. C. Gauthier, M. Ashman, *Appl. Opt.* **37**, 6421 (1998).
14. L. Allen, M. W. Beijersbergen, R. J. C. Spreeuw, J. P. Woerdman, *Phys. Rev. A* **45**, 8185 (1992).
15. M. P. MacDonald *et al.*, *Opt. Commun.* **201**, 21 (2002).
16. R. Piestun, Y. Y. Schechner, J. Shamir, *J. Opt. Soc. Am. A* **17**, 294 (2000).
17. Y. Y. Schechner, R. Piestun, J. Shamir, *Phys. Rev. E* **54**, R50 (1996).
18. A. A. Tovar, *J. Opt. Soc. Am. A* **17**, 2010 (2000).
19. B. A. Garetz, *J. Opt. Soc. Am.* **71**, 609 (1981).
20. A. E. Chiou, W. Wang, G. J. Sonek, J. Hong, M. W. Berns, *Opt. Commun.* **133**, 7 (1997).
21. S. Kuhr *et al.*, *Science*, **293**, 278 (2001).
22. F. Bretenaker, A. Le Floch., *Phys. Rev. Lett.* **65**, 2316 (1990).
23. M. M. Burns, J. M. Fournier, J. A. Golovchenko, *Science* **249**, 749 (1990).
24. We thank the UK Engineering and Physical Sciences Research Council, The Royal Society Paul Instrument Fund, and the Medical Research Council for supporting this research and W. C. K. Poon for useful discussions. K.V.S. acknowledges the support of CONACYT, Mexico and S. Chávez-Cerda.

7 January 2002; accepted 25 March 2002

Single-Molecule Optomechanical Cycle

Thorsten Hugel,[1] Nolan B. Holland,[1]* Anna Cattani,[2] Luis Moroder,[2] Markus Seitz,[1] Hermann E. Gaub[1]†

Light-powered molecular machines are conjectured to be essential constituents of future nanoscale devices. As a model for such systems, we have synthesized a polymer of bistable photosensitive azobenzenes. Individual polymers were investigated by single-molecule force spectroscopy in combination with optical excitation in total internal reflection. We were able to optically lengthen and contract individual polymers by switching the azo groups between their trans and cis configurations. The polymer was found to contract against an external force acting along the polymer backbone, thus delivering mechanical work. As a proof of principle, the polymer was operated in a periodic mode, demonstrating for the first time optomechanical energy conversion in a single-molecule device.

Nanomechanical devices or molecular machines will, for a broad range of applications, most likely be powered by light or other kinds of electromagnetic radiation (*1–4*). The dominant reasons are ease of addressability, picosecond reaction times to external stimuli, and compatibility with a broad range of ambient substances, such as solvents, electrolytes, gases, or vacuum. One of the key challenges, not only in the development phase but also in operation, is the need to interface such nanometer-sized or molecular devices with the macroscopic world. Single-molecule force spectroscopy by atomic force microscope (AFM) techniques has in the past proven to be an extremely successful strategy (*5–16*). Successful attempts to use an AFM tip to guide the activity of enzymes have paved the road toward a molecular machine tool (*17*).

We now combine single-molecule mechanics with optics to excite an ensemble of molecules and mechanically select an individual molecule from this ensemble. As the photoactive system, we used a polymer of azobenzene units (Fig. 1). This well-studied chromophore, which can be reversibly

[1]Lehrstuhl für Angewandte Physik & Center for Nanoscience, Ludwig-Maximilians Universität, Amalienstrasse 54, 80799 München, Germany. [2]Max-Planck-Institut für Biochemie, Am Klopferspitz 18 a, 82152 Martinsried, Germany.

*Present address: Department of Physiology and Biophysics, Case Western Reserve University, 10900 Euclid Avenue, Cleveland, OH 44106, USA.
†To whom correspondence should be addressed.

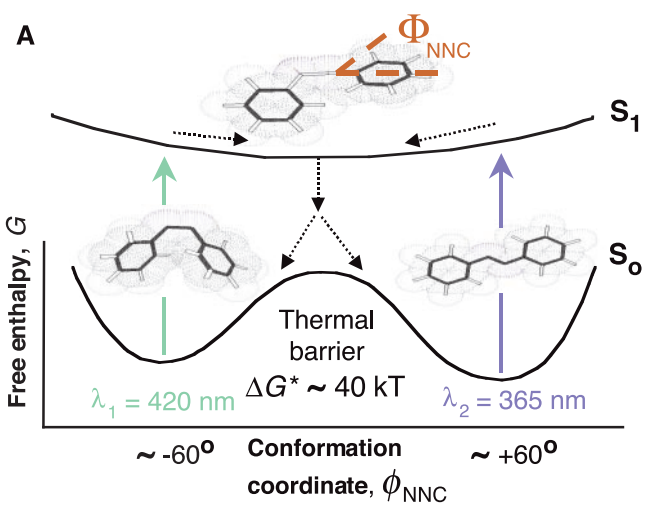

Fig. 1. (**A**) Schematics of a cut through the potential energy landscape of the reversible azobenzene cis-trans transition along the inversion pathway. The relevant conformational coordinate is the bond angle, Φ_{NNC}, which changes from about −60° to +60° for an in-plane transition of the right phenyl ring from the cis to the trans position (*49*). The transition can be induced by optical excitation from the singulette electronic ground state S_0 to the first excited singulett state S_1 (cis form, λ_1 = 420 nm; trans form, λ_2 = 365 nm). Typically, the trans form is thermally favored [the shown graph is based on previous theoretical (*35*) and experimental (*36*, *37*) data]. (**B**) Synthesis of polyazobenzene peptides (*40*).

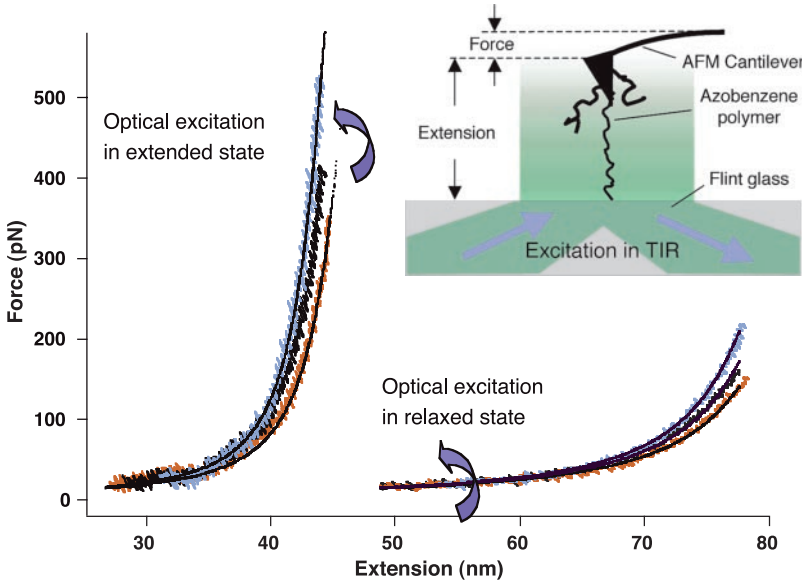

Fig. 2. Traces at right are force extension traces (*50*) of a single polyazopeptide. The experiment started with a polymer in a nondefined initial configurationally mixed state (black trace, L = 86.5 nm). By the application of five 420-nm pulses, the polymer was switched to the saturated trans state and lengthened by ~1.4 nm (red trace). After five pulses at 365 nm, the same molecule shortened by ΔL = 2.8 nm. The contour lengths L of the stretched polymer strands were obtained from a fit to the extended worm-like chain (WLC) model using a persistence length of L_p = 0.5 nm and a polymer segment elasticity of E = 20,000 pN. In the traces at left, a single polyazopeptide strand was shortened against an external force. First, the strand was driven into the trans state by five pulses at 420 nm and then it was stretched to a force of about 350 pN (red trace). Application of one pulse at 365 nm at constant tip/sample separation resulted in a shortening by about 1.1 nm (black trace). Two further pulses resulted in an additional shortening by 0.8 nm (blue trace). Because five additional pulses did not result in further shortening, the polymer was assumed to be in the saturated cis state. (Inset) Schematics of the experimental setup. TIR, total internal reflection. Single-molecule force spectroscopy was performed with a modified instrument from Asylum Research (Santa Barbara, CA) (*40*).

switched at two different wavelengths between an extended trans and a shorter cis configuration (*18*, *19*), has been the basis for many experiments, such as light-driven ion transport through membranes (*20*). It has frequently been used in synthetic photoresponsive systems, regulating the geometry and function of biomolecules (*21*–*23*), organic materials (*24*–*27*), and supramolecular complexes (*28*–*30*). Photomechanical effects have been demonstrated for azobenzene polymers in bulk (*31*–*34*). The potential energy landscape of azobenzene (Fig. 1A) has been determined in ab initio calculations and experimentally probed by spectroscopy (*35*–*37*). The conformational flexibility required for reversible optical switching is retained in a polypeptide backbone (Fig. 1B) (*38*, *39*). To ensure stable attachment, the polymer end groups were covalently coupled to both the AFM tip and a supporting glass slide by heterobifunctional chemistry (*40*).

Total internal reflection geometry was chosen for the optical excitation to avoid thermomechanical disturbances due to absorption of the optical stimulus by the cantilever (*41*). At a length of the cantilever tip of several micrometers, the penetration depth of the evanescent field of about wavelength $(\lambda)/2\pi \approx 50$ nm is short enough to prevent excitation of the cantilever itself (*42*). Thus, the polymer length should not need to exceed this value in order to be excited. We directly focused the light from a high-pressure mercury lamp onto the edge of a microscope slide at an aperture below the critical angle of total internal reflection, so that the slide acted as a wave guide. Because dimethyl sulfoxide (DMSO) was chosen as the solvent, high-refractive-index flint glass with high transmission in the ultraviolet was used. Control experiments showed that in this experimental setup, thermal effects on single polymer elasticity were negligible (*40*).

Figure 2 shows the realization of the concept discussed above. The right set of traces shows the changes in the mechanical compliance of a single azobenzene polymer resulting from optical switching between its cis and trans configurations at zero force. First, the polymer was measured in its initial configurationally mixed state (black trace). Then, five pulses at λ = 420 nm were applied that drove the polymer into the saturated trans state (*43*). The polymer was stretched and the red trace was measured, revealing a marked lengthening of the polymer. The polymer was relaxed again, and five pulses of λ = 365 nm were applied to drive the polymer into the saturated cis state (*43*). As a result, the polymer exhibited marked shortening (blue trace). Such cycles may be repeated several times before the polymer or its attachment ruptures. We observed that the stability is drastically reduced if the polymer is kept at elevated forces for prolonged times.

The trans monomer length, that is, the max-

imum end-end distance of a single azotripeptide monomer, was calculated with the INSIGHT II software package to be $l_{trans} \approx 1.9$ nm. The fitted contour length of the polymer, $L \approx 88$ nm, equals $n \approx 47$ azotripeptide units. The length difference for a single azobenzene unit in the cis and the trans state can be taken from ab initio quantum mechanical calculations as $\Delta d^{4-4'} \approx 0.25$ nm (*35*). Considering that effectively only 55% of the azobenzenes change their configuration upon cis-trans switching, a maximum length change of $\Delta L \approx 6$ nm may be obtained by optical pumping at 365 nm. Our measured length change in DMSO of 2.8 nm stays below this upper limit (*40*). The difference may reflect the fact that parts of the polymer chain are not excited by the evanescent field. Also, intrinsic viscosity measurements on azobenzene polymers have shown the largest effects of optical excitation on the end-end distance of the polymer coils in solution, when the photoactive units were connected by stiff rather than flexible chain segments (*32*, *44*). In our experiments, the polymer chains are fixed between tip and substrate and are stretched beyond the coil regime. Although this geometry is thus more comparable with photoactive bulk polymer networks, which may show considerable length changes upon optical switching (*45*), the remaining conformational freedom of the polypeptide backbone may compensate for some of the azobenzene shortening by rotations around single backbone bonds (*38*, *46*).

Although bulk measurements on azobenzene containing peptides give a thermal relaxation time of several hours at room temperature (*38*), we did not observe the thermal back reaction within the time span of the experiments. Thus, the thermal and forced conversion paths do not coincide. Moreover, the left set of traces in Fig. 2 shows that switching is possible even against an external force. Only at forces above 500 pN have we not observed the optical trans-cis isomerization reaction so far. These experiments show that we can (i) handle and manipulate an individual polyazopeptide, (ii) mechanically measure its length and its compliance, (iii) optically excite this polymer and pump it into a predominantly cis or predominantly trans state, and (iv) detect this transition mechanically.

How could we use such a polymer to convert optical excitation into mechanical work? In Fig. 3A, a gedankenexperiment is sketched, in which a polymer is prestretched with a bias force F_0. A weight is added, stretching the compliant molecule to F_1. Then the polymer is optically contracted, lifting the weight and thereby doing mechanical work. The weight is removed and the polymer is optically switched back, so that the cycle may start again.

This gedankenexperiment was put into reality with the experimental cycle shown in Fig. 3B, which describes the force extension plot. The mechanical branches are determined by the molecular extensibilities of the polymer, which are well described by the WLC model. The slopes of the optical branches of the cycle are determined by the stiffness of the cantilever. Upon optical contraction of the polymer, the force increases because the contracting polymer pulls down the cantilever (similar logic holds for the optical expansion). The light-driven mechanical work of contraction is given by the blue area.

The experimental data are shown in Fig. 4. An individual azopolymer was first lengthened by five pulses with $\lambda = 420$ nm at a force of 80 pN (I) and then expanded mechanically to a restoring force of 200 pN (II). Then five pulses at $\lambda = 365$ nm were applied, resulting in a contraction of the polymer against the external force (III). Then the force on the polymer was reduced to 85 pN (IV). Finally, the cycle was completed by applying five pulses at $\lambda = 420$ nm, resulting in an optical expansion of the molecule to its original length. From the cycle, we may estimate the quantum efficiency of the trans-cis switching process. The mechanical work performed by the azobenzene polymer strand upon its transition from II to III is simply given as $W_{mech} = \Delta L \times F_{II \rightarrow III}$; that is, here $W_{mech} \approx 0.22$ nm $\times$ 205 pN $\approx 4.5 \times 10^{-20}$ J. Because this mechanical work at the molecular level results from a macroscopic optical excitation ($E_{opt} \approx 10$ mJ), the real quantum efficiency of optomechanical switching for the given cycle in our AFM setup is only on the order of 10^{-18}. However, a maximum efficiency of the optome-

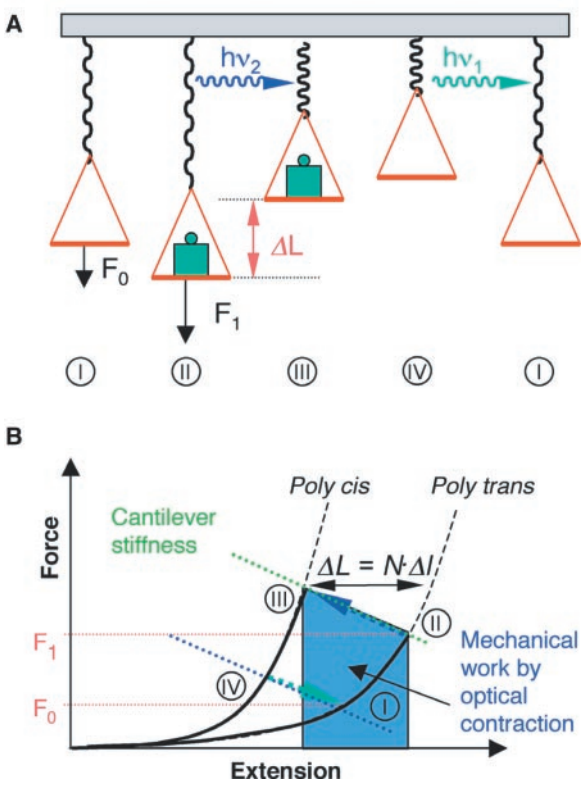

Fig. 3. Schematics of the single-molecule operating cycle. Points I through IV in (**A**) represent the four states of an operating cycle based on a polymer consisting of repeating segments exhibiting a reversible transition from a short to an extended configuration, and vice versa. $h\nu_1$ and $h\nu_2$ indicate the energy of excitation photons (of frequencies $\nu 1$ and $\nu 2$, respectively). (**B**) The corresponding force extension cycle starts at point I on the force-distance curve of the long polymer configuration, at which the polymer is in its extended configuration. When an external load is applied to the polymer, it will follow the force-distance curve of the extended polymer configuration up to point II, where the system is switched back to its short configuration, point III, by an external stimulus (here, light). The removal of the load results in (reversible) relaxation of the polymer band, which brings the system to point IV. From there it is switched back to the starting point of the cycle by another external stimulus. The work output of the system is the mechanical energy related to the contraction $\Delta L = N \times \Delta l$ of the polymer band against the external load. The external input needed to perform this mechanical work is the energy of the external stimulus (plus the energy needed to apply the load). As for any thermodynamic cycle, the efficiency of energy conversion η can then be defined by the ratio W_{out}/W_{in}.

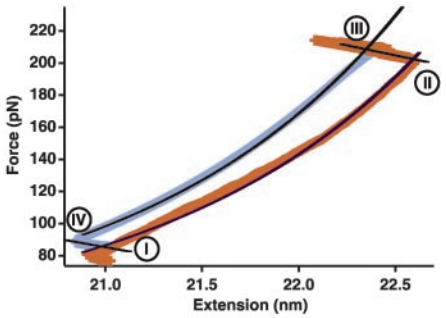

Fig. 4. Experimental realization of the single-molecule operating cycle with polyazopeptides. Five 420-nm flashes drive the polymer into its extended (mainly trans) state (I) at low force (here, 100 pN), and it is then further stretched (red trace). In the stretched state (II), at which a mechanical force $F = 200$ pN acts on the extended polymer, three 365-nm pulses were applied, which shortens the molecule (trans-cis transition). The force increases during the transition to the shortened state, as an effect of the cantilever stiffness (dotted line), to point III. Upon release of the mechanical stress, the polymer follows the blue trace to point IV, from which a new cycle can be started by switching the shortened configuration to the extended state. The black lines are extended WLC fits, which give contour lengths of 24.8 and 24.5 nm, respectively.

chanical energy conversion at a molecular level can be estimated as $\eta \approx 0.1$ from the left trace in Fig. 2, if it is assumed that each switching of a single azobenzene unit is initiated by a single photon carrying an energy of $E_{exc} = 5.5 \times 10^{-19}$ J ($\lambda = 365$ nm) (*47*).

In any case, an increased conversion efficiency will promote the application of future mechano-optical devices in high-density configurations, and the use of such molecular hybrids in more complex settings will be stimulated by improvements in their stability and their ability to interact with other components.

References and Notes

1. V. Balzani, A. Credi, F. M. Raymo, J. F. Stoddart, *Angew. Chem. Int. Ed.* **39**, 3348 (2000).
2. B. L. Feringa, R. A. van Delden, N. Koumura, E. M. Geertsema, *Chem. Rev.* **100**, 1789 (2000).
3. J. P. Collin, P. Gaviña, V. Heitz, J. P. Sauvage, *Eur. J. Inorg. Chem.* **1998**, 1 (1998).
4. J. M. Lehn, *Supramolecular Chemistry: Concepts and Perspectives* (Wiley-VCH, Weinheim, Germany, 1995).
5. G. U. Lee, D. A. Kidwell, R. J. Colton, *Langmuir* **10**, 354 (1994).
6. V. T. Moy, E.-L. Florin, H. E. Gaub, *Colloids Surf.* **93**, 343 (1994).
7. S. S. Wong, E. Joselevich, A. T. Woolley, C. L. Cheung, C. M. Lieber, *Nature* **394**, 52 (1998).
8. M. Rief, F. Oesterhelt, B. Heymann, H. E. Gaub, *Science* **275**, 1295 (1997).
9. M. Rief, M. Gautel, F. Oesterhelt, J. M. Fernandez, H. E. Gaub, *Science* **276**, 1109 (1997).
10. A. Janshoff, M. Neitzert, Y. Oberdörfer, H. Fuchs, *Angew. Chem. Int. Ed.* **39**, 3212 (2000).
11. H. Clausen-Schaumann, M. Seitz, R. Krautbauer, H. Gaub, *Curr. Opin. Chem. Biol.* **4**, 524 (2000).
12. T. Hugel, M. Seitz, *Macromol. Rapid Commun.* **22**, 989 (2001).
13. B. L. Smith *et al.*, *Nature* **399**, 761 (1999).
14. A. F. Oberhauser, P. E. Marszalek, H. P. Erickson, J. M. Fernandez, *Nature* **393**, 181 (1998).
15. F. Oesterhelt *et al.*, *Science* **288**, 143 (2000).
16. G. Binnig, C. F. Quate, C. Gerber, *Phys. Rev. Lett.* **56**, 930 (1986).
17. H. Clausen-Schaumann, M. Grandbois, H. E. Gaub, *Adv. Mater.* **10**, 949 (1998).
18. G. S. Hartley, *Nature* **140**, 281 (1937).
19. H. Rau, in *Photochromism: Molecules and Systems*, H. Dürr, H. Bouas-Laurent, Eds. (Elsevier, Amsterdam, 1990), chap. 4.
20. S. Shinkai, O. Manabe, *Top. Curr. Chem.* **121**, 76 (1984).
21. I. Willner, *Acc. Chem. Res.* **30**, 347 (1997).
22. L. Ulysse, J. Cubillos, J. Chmielewski, *J. Am. Chem. Soc.* **117**, 8466 (1995).
23. H. Asanuma, T. Ito, T. Yoshida, X. Liang, M. Komiyama, *Angew. Chem. Int. Ed.* **38**, 2393 (1999).
24. B. L. Feringa, W. F. Jager, B. de Lange, *Tetrahedron* **49**, 8267 (1993).
25. N. Tamai, H. Miyasaka, *Chem. Rev.* **100**, 1875 (2000).
26. G. S. Kumar, D. C. Neckers, *Chem. Rev.* **89**, 1915 (1989).
27. M. Irie, *Adv. Polym. Sci.* **94**, 27 (1990).
28. F. Vögtle, *Supramolecular Chemistry* (Wiley, New York, 1991).
29. F. Würthner, J. Rebek Jr., *J. Chem. Soc. Perkin Trans. 2* **1995**, 1727 (1995).
30. A. Archut, G. C. Azzellini, V. Balzani, L. De Cola, F. Vögtle, *J. Am. Chem. Soc.* **120**, 12187 (1998).
31. C. D. Eisenbach, *Polymer* **21**, 1175 (1980).
32. H. S. Blair, H. I. Pogue, E. Riordan, *Polymer* **21**, 1195 (1980).
33. L. A. Strzegowski, M. B. Martinez, D. C. Gowda, D. W. Urry, D. A. Tirrell, *J. Am. Chem. Soc.* **116**, 813 (1994).
34. F. Lagugné Labarthet *et al.*, *Phys. Chem. Chem. Phys.* **2**, 5154 (2000).
35. S. Monti, G. Orlandi, P. Palmieri, *Chem. Phys.* **71**, 87 (1982).
36. H. Rau, *J. Photochem.* **26**, 221 (1984).
37. T. Nägele, R. Hoche, W. Zinth, J. Wachtveitl, *Chem. Phys. Lett.* **272**, 489 (1997).
38. C. Renner, J. Cramer, R. Behrendt, L. Moroder, *Biopolymers* **54**, 501 (2000).
39. R. Behrendt *et al.*, *Angew. Chem. Intl. Ed.* **38**, 2771 (1999).
40. Molecular synthesis and spectroscopic details of the azobenzene polypeptides, as well as further information on the optomechanical AFM experiments, can be found on *Science* Online at www.sciencemag.org/cgi/content/full/296/5570/1103/DC1.
41. J. Fritz *et al.*, *Science* **288**, 316 (2000).
42. D. Axelrod, T. P. Burghardt, N. L. Thompson, *Annu. Rev. Biophys. Bioeng.* **13**, 247 (1984).
43. Because of the spectral overlap of the excitations of cis and trans configurations, the configuration average cannot be shifted entirely upon optical pumping. The respective resulting maximum populations are ~80% in the trans and 75% in the cis state (*38*).
44. M. Irie, Y. Hirano, S. Hashimoto, K. Hayashi, *Macromolecules* **14**, 262 (1981).
45. H. Finkelmann, E. Nishikawa, G. G. Pereira, M. Warner, *Phys. Rev. Lett.* **87**, 015501 (2001).
46. The maximum change of the azobenzene end-end distance by $\Delta d^{4-4'} \approx 0.25$ nm would then not be fully accounted for in the shortening of the polymer along the stretching direction. The assumption that full optical excitation of the polymer results in maximum trans-cis switching yields an average shortening by $\Delta l = 0.11$ nm per tripeptide monomer unit along the *z* axis.
47. Next to losses by dissipation of optical excitation energy, the spectral overlap causing incomplete trans-cis switching and the quantum yield of its electronical excitation are the intrinsic limiting factors of the azobenzene system.
48. J. M. Robertson, *J. Chem. Soc.* **1939**, 232 (1939).
49. Ab initio calculations (*35*) gave an angle of $\phi_{NNC} \approx -54°$ (Fig. 1A) for the cis configuration and $\phi_{NNC} \approx 66°$ for the trans configuration. This corresponds to x-ray and nuclear magnetic resonance experiments that gave values for the cis configuration of –55° and –50°, respectively (*38*, *48*).
50. Force extension traces were obtained from the deflection piezopath signal as described elsewhere (*12*). Indentation traces were taken before and after each set of traces to determine the exact position of the surface and therefore to allow correction for drift in the deflection and piezo signal.

51. Helpful discussions with J. Brauman, H. Grubmüller, D. Oesterhelt, C. Renner, and W. Zinth as well as technical support from AsylumResearch are gratefully acknowledged. Supported by the Deutsche Forschungsgemeinschaft, the Humboldt Foundation, and the Fonds der Chemischen Industrie.

15 January 2002; accepted 25 March 2002

An Efficient Two-Photon–Generated Photoacid Applied to Positive-Tone 3D Microfabrication

Wenhui Zhou,[1] Stephen M. Kuebler,[1] Kevin L. Braun,[1] Tianyue Yu,[3] J. Kevin Cammack,[1] Christopher K. Ober,[3]* Joseph W. Perry,[1,2]* Seth R. Marder[1,2]*

A two-photon–activatable photoacid generator, based on a *bis*[(diarylamino) styryl]benzene core with covalently attached sulfonium moieties, has been synthesized. The photoacid generator has both a large two-photon absorption cross section ($\delta = 690 \times 10^{-50}$ centimeter^4 second per photon) and a high quantum yield for the photochemical generation of acid ($\phi_{H^+} = 0.5$). Under near-infrared laser irradiation, the molecule produces acid after two-photon excitation and initiates the polymerization of epoxides at an incident intensity that is one to two orders of magnitude lower than that needed for conventional ultraviolet-sensitive initiators. This photoacid generator was used in conjunction with a positive-tone chemically amplified resist for the fabrication of a three-dimensional (3D) microchannel structure.

The process of two-photon absorption (TPA) is currently being examined for a variety of applications, including three-dimensional (3D) microfabrication (*1*–*4*), ultra-high-density optical data storage (*5*), biological imaging (*6*), and the controlled release of biologically relevant species (*7*). Conventional ultraviolet (UV)–sensitive photoacid generators (PAGs), such as diaryliodonium and triarylsulfonium cations, have been used for two-photon microfabrication (*8*). However, the TPA cross sections, δ, of these initiators are typically very small ($\delta \leq 10 \times 10^{-50}$ cm^4 s per photon), and as a result they exhibit low two-photon sensitivity. Resins containing these initiators can be patterned only by means of long exposure times and high excitation intensities that frequently result in damage to the structure. Higher reliability and faster write speeds would be facilitated by molecules offering a large product of δ and the photochemical quantum yield ϕ_{H^+}. The design of highly photosensitive two-photon initiators requires (i) a chromophoric group with a large δ, such as two electron donors bridged by a π-conjugated system (a D-π-D structure) (*9*, *10*); (ii) a functionality that can generate the initiating species with high efficiency, such as those in UV initiators; and (iii) a mechanism through which excitation of the chromophore leads to activation of the chemical functionality, such as an electron transfer process (*2*). Here we describe the development of a high-sensitiv-